Influence of water layer thickness on hard tissue ablation with pulsed CO_2 laser

Xianzeng Zhang
Zhenlin Zhan
Haishan Liu
Haibin Zhao
Shusen Xie
Qing Ye

Influence of water layer thickness on hard tissue ablation with pulsed CO$_2$ laser

Xianzeng Zhang,[a] **Zhenlin Zhan,**[a] **Haishan Liu,**[a] **Haibin Zhao,**[a] **Shusen Xie,**[a] **and Qing Ye**[b]
[a]Fujian Normal University, Institute of Laser and Optoelectronics Technology, Fujian Provincial Key Laboratory for Photonics Technology, and Key Laboratory of OptoElectronic Science and Technology for Medicine of Ministry of Education, Fuzhou, China
[b]Provincial Clinical College of Fujian Medical University, Fujian Provincial Hospital, Department of Otolaryngology, Fuzhou, China

Abstract. The theory of hard tissue ablation reported for IR lasers is based on a process of thermomechanical interaction, which is explained by the absorption of the radiation in the water component of the tissue. The micro-explosion of the water is the cause of tissue fragments being blasted from hard tissue. The aim of this study is to evaluate the influence of the interdependence of water layer thickness and incident radiant exposure on ablation performance. A total of 282 specimens of bovine shank bone were irradiated with a pulse CO$_2$ laser. Irradiation was carried out in groups: without a water layer and with a static water layer of thickness ranging from 0.2 to 1.2 mm. Each group was subdivided into five subgroups for different radiant exposures ranging from 18 to 84 J/cm^2, respectively. The incision geometry, surface morphology, and microstructure of the cut walls as well as thermal injury were examined as a function of the water layer thickness at different radiant exposures. Our results demonstrate that the additional water layer is actually a mediator of laser–tissue interaction. There exists a critical thickness of water layer for a given radiant exposure, at which the additional water layer plays multiple roles, not only acting as a cleaner to produce a clean cut but also as a coolant to prevent bone heating and reduce thermal injury, but also helping to improve the regularity of the cut shape, smooth the cut surface, and enhance ablation rate and efficiency. The results suggest that desired ablation results depend on optimal selection of both water layer thickness and radiant exposure. © *2012 Society of Photo-Optical Instrumentation Engineers (SPIE).* [DOI: 10.1117/1.JBO.17.3.038003]

Keywords: CO$_2$ laser irradiation; ablation; hard tissue; water-mediated ablation.

Paper 11676 received Nov. 20, 2011; revised manuscript received Jan. 17, 2012; accepted for publication Jan. 20, 2012; published online Mar. 26, 2012.

1 Introduction

Osteotomy with infrared (IR) lasers has several advantages over drills and oscillating saws, the usual mechanical tools. The noncontact application of a focused laser beam offers arbitrary intricate cut geometry, especially when combined with advanced computer control, and permits more precise and comfortable removal of hard tissue. There is no traumatic vibration, bone dust, or metal abrasion in the incision during laser osteotomy. Aseptic and hemostatic effects can be expected by application of some laser systems.[1–4] A number of studies have been done to characterize bone tissue ablation with various of wavelengths and pulse durations.[5–13] Since the wavelengths of CO$_2$ (9.3 to 10.6 μm), Er:YAG (2.94 μm), and Er,Cr:YSGG (2.78 μm) lasers coincide with the strong absorption peaks of two main components of bone tissue—that is, hydroxyapatite (65% of the weight of bone) and water (10 to 15% of the weight of bone)—they are the most suitable candidates for bone surgery.[7,13,14] The primary mechanism reported for IR lasers is thermomechanical: light absorption by water and/or mineral bone components in thin tissue layer could heat interstitial water and lead to internal pressure that reaches the ultimate tensile strength of the tissue, consequently resulting in explosive removal of the outer layers of bone tissue.[3,12,14]

It is well known that dehydration of the irradiated tissue caused by rapid temperature increase during laser—tissue interaction leads to thermal damage to surrounding tissue, resulting in carbonization, cracking, and a loss of effectiveness. Furthermore, temperature elevation between 44 and 47°C may lead to bony tissue necrosis.[15] In clinical practice, an external water spray additionally has to be provided as a cooling agent to make it possible to reduce the thermal stress on the surrounding tissues and prevent damage.[16,17] At the same time, however, it is surprising in the context that supplying water externally also serves to increase ablation rate and efficiency, improve surface morphology, alter chemical composition, and enhance adhesion to restorative materials.[1,18–20] Although the role of external water in ablation has not yet been demonstrated clearly, it is clear that externally supplied water, rather than water contained in the tissue, significantly influences the effectiveness of the ablation process.[18]

However, the external water effects mentioned above in laser ablation are based mainly on the interaction of dental hard tissue with erbium lasers, including Er:YAG (2.94 μm), Er:YSGG (2.79 μm), and Er,Cr:YSGG (2.78 μm) lasers. The room temperature absorption coefficient of water, μ_a, is 12480 cm^{-1} at 2.94 μm and 4180 cm^{-1} at 2.79 μm,[21] which is an order of magnitude larger than that of enamel ($\mu_a = 800$ cm^{-1} at 2.94 μm and 480 cm^{-1} at 2.79 μm).[22] A systematic study of the influence of externally supplied water on bone tissue ablation with pulsed CO$_2$ laser has not yet been reported. Unlike erbium lasers whose main absorber is water, the absorption of pure hydroxyapatite at

Address all correspondence to: Shusen Xie, Fujian Normal University, Institute of Laser and Optoelectronics Technology, Fujian Provincial Key Laboratory for Photonics Technology, and Key Laboratory of OptoElectronic Science and Technology for Medicine of Ministry of Education, Fuzhou, China. Tel: 0860059183465373; Fax: 0860059183465373; E-mail: xzzhang@fjnu.edu.cn.

CO_2 laser wavelengths ranges from 3500 to 5500 cm^{-1}, which is 4 to 9 times higher than that for H_2O.[23] We expect to observe some new features of water-mediated bone tissue ablation with pulsed CO_2 laser associated with this difference through the present study. Furthermore, although a variety of basic investigations on water effects with this procedure using erbium lasers have been done, and different hypotheses including cavitation bubbles, hydrokinetic effect, and apatite crystalline fragments have been presented for evaluation,[24,25] the actual mechanism of interaction among the water spray or water layer, the laser irradiation, and the hard tissues is not yet clearly understood and is somewhat controversial. Moreover, it is still a question whether the already reported hypotheses based on erbium lasers are suitable to explain the process of water-mediated hard tissue ablation with CO_2 laser.

The present work first evaluated the influence of water layers with different thicknesses on hard bone tissue ablation at various radiant exposures with a wavelength of 10.6 μm. Ablation performance, including ablation surface morphology, cut geometry, thermal injury, and microstructure, were examined as a function of water layer thickness at various incident radiant exposures. The possible roles of the additional water layer in the water-mediated ablation process and related mechanisms were also discussed.

2 Materials and Methods

Fresh bovine shank bone obtained no later than 6 h postmortem from a local slaughterhouse was used for in vitro laser-tissue ablation experiments. The bone specimens were rinsed in tap water to remove hemocytes after the connective tissue and periosteum were peeled away with a razor blade. Then the sample was cut into rectangular blocks ($\sim 2 \times 4$ cm with original compacta thickness) with a diamond saw. To obtain a flat surface, the sample surface was polished using sandpaper with a grain size of 30 μm followed by ultrasonic cleaning to remove the smear layer, and then the prepared samples were stored in a saline solution at 4°C prior to experimentation to prevent dehydration.

Laser light emitted from a pulsed CO_2 laser (Sharplan 30C, Laser Industries LTD, Israel) operating at 10.6 μm with pulse duration of about 100 μs was transmitted though an articulated-mirror-arm system and focused to a spot size of about 400 μm on the bone sample surface directly with a 125-mm lens, which was determined at $1/e^2$ intensity level measured using the "knife-edge" method. The radiant exposure delivered to the tissue was set to predetermined values between 18 and 84 J/cm^2, which was confirmed by reading the laser pulsed energy (NOVA II, Orphir, Israel) with a pyroelectric detector and dividing the beam area. The repetition rate was 60 Hz. The bone sample was fixed on a customized holder that was put on a PC-controlled motorized linear drive stage and moved repeatedly through the focused beam. The geometrical pulse overlap factor n can be defined by the formula $n = fw/v$. The equivalent pulse number acting effectively at every point along the incision can be calculated by the product of pulse overlap factor and scanning repetition times. In the present study, the moving rate and scanning repetition times were set at 12 mm/s and 5, respectively, which means five pulses acted effectively at every point along the incision. To evaluate the influence of the thickness of the water layer applied to the bone sample surface and the incident radiant exposure on ablation effects, the bone samples were divided into seven groups randomly for laser ablation under dry conditions (without water layer) and wet conditions with water layer thicknesses ranging from 0.2 to 1.2 mm on the tissue surface before laser irradiation, respectively, and then each group was subdivided into five subgroups for radiant exposures of 18, 32, 50, 70, and 84 J/cm^2, respectively. A schematic presentation of laser irradiation on bovine shank bone in the experiment is shown in Fig. 1.

To precisely control the thickness of the water layer applied to the bone sample surface, a novel device based on the principle of connected vessels was designed as shown in Fig. 2(a). Two glass containers with inner diameters of 9.5 cm (A) and 1.5 cm (B) were connected with a tube. A customized sample holder was fixed in container A to ensure that the distance between the top surface of tissue sample and the bottom of the container was the same for all the tissue samples. By moving container B up and down, the thickness of the water layer on the top of the tissue sample surface can be calculated by the formula $h = \frac{d_B^2}{d_A^2 + d_B^2} y$, where d_A and d_B are the inner diameter of container A and B, and y is the moving displacement of container B. For example, if container B was moved up or down 1 mm, the water level of container A would rise or descend about 1/41 mm (about 24 μm).

To evaluate the effectiveness of the connected vessel device (CVD), a baseline was determined where the tissue surface fixed in container A and the water surface in container B are on a horizontal plane, and then container B was moved up consistently in steps of 2 mm. At each movement, the thickness of the water
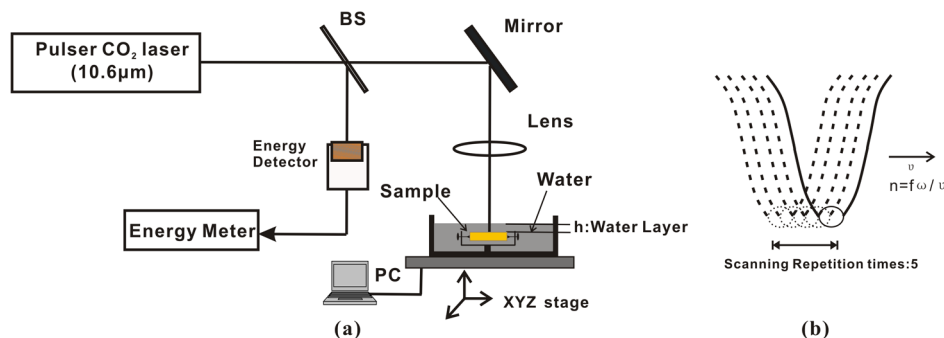

Fig. 1 Schematic presentation of laser irradiation on bovine shank bone in the experiment: (a) experimental setup; (b) the number of pulses acting effectively at every point along the incision can be defined as the product of the pulse overlap factor n and the scanning repetition times. Pulse overlap factor can be defined as $n = fw/v$, which contains the pulse repetition rate f, the beam focus radius at $1/e^2$ level w, and the moving rate v. The scanning repetition time is the number of times the laser beam scans the tissue surface.
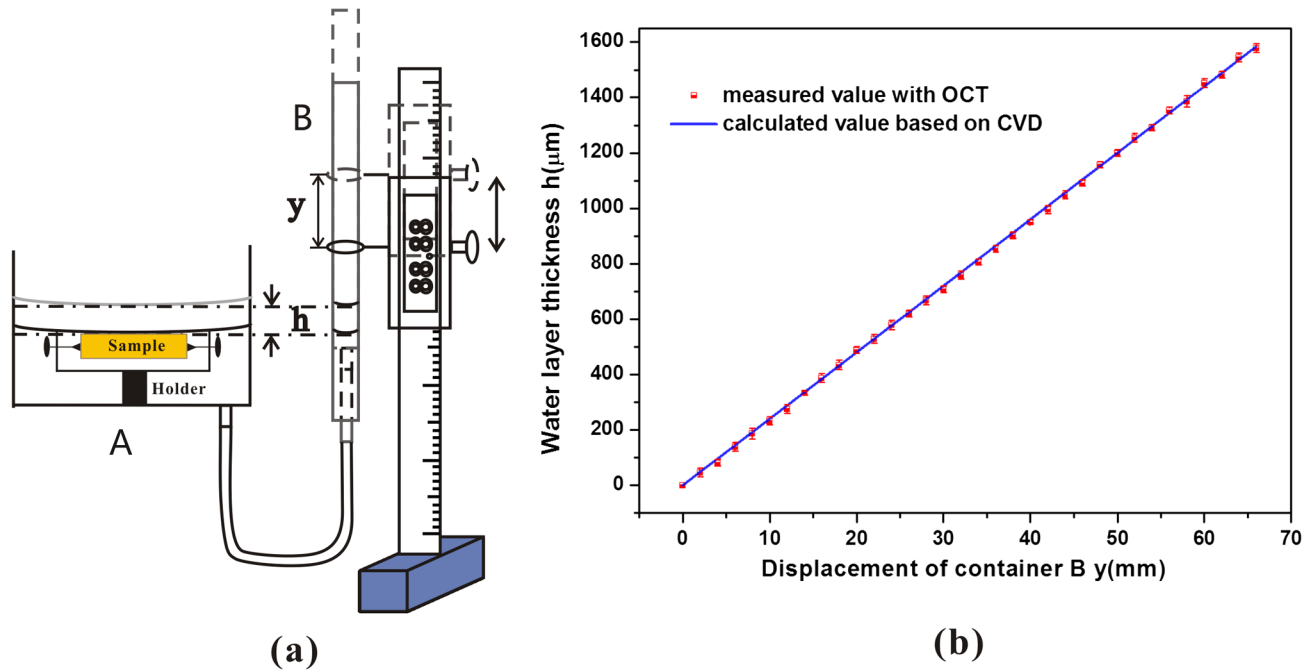
Fig. 2 (a) Novel device based on the principle of connected vessels to control the water layer thickness applied to tissue surface. (b) Good match between calculated value of water layer thickness based on connected vessel device (CVD) and measured value with OCT. The error bars are standard deviation of the data ($n = 5$).

layer on the tissue surface was measured with an optical coherent tomography (OCT, MOPTIM Co., China) system with lateral and axial resolutions of $\sim$10 μm. As shown in Fig. 2(b), the measured value presented a good consistency with the value calculated by the above formula, which suggested that the CVD can control the water layer thickness precisely.

After irradiation, the morphological changes to the tissue sample were examined by stereomicroscopy first, and then cross-section imaging of the incision was acquired with OCT. The geometry of the cross section of the incision, including width and depth, were measured based upon OCT images from self-compiled software. Afterwards, the treated bone samples were divided randomly into two groups for histological analysis and scanning electron microscopy (SEM) examination. For histological analysis, the bone sample was fixed in 10% neutral buffered formalin, decalcified in HNO_3 solution for 5 days, and then embedded in paraffin. Serial sections 4 to 5 μm thick were cut transversely to the laser cuts from the embedded sample, mounted on 1- by 3-in. glass slides, and stained with hematoxylin and eosin-y (H&E). Histological changes were observed with light microscopy (BX40-12J-02, Olympus, Japan). The thickness of the thermal injury zone was measured at three points: the base of the cut and the midpoint of each side of the cut wall, as shown in Fig. 3. For SEM groups, the specimens were dried in an exhaust system, mounted on stubs with their treated surfaces face up, sputter-coated with gold, and examined with SEM (JSM-6380LV, Japan) operating at 15 kV.

Measured values of crater geometry including width and depth, and the thickness of the thermal injury zones at various water layer thicknesses with different radiant exposures were summarized and displayed graphically by means and corresponding standard deviations. Statistical evaluation was performed with a two-tailed t-test. A p-value of $p \leq 0.05$ indicates a statistically significant effect of the corresponding factor on

the measured value. All statistical analysis was carried out using SPSS statistical analysis software, version 13.0.

3 Results

3.1 Morphological Changes

Figure 4 presents top-view stereomicroscope and cross-section OCT images of an ablation cut created on a bone sample by pulsed CO_2 laser at 18 and 84 J/cm^2 without and with a water layer of 0.8 mm, respectively. The cut shapes presented cut profiles with regular V-shaped cross sections for all groups of bone samples in the study. In the dry condition [Figs. 4(A), 4(a), 4(B), and 4(b)], the cut showed irregular surface deformation with a layer of black char formation and brown tissue denaturalization distributing along the edge of the cut (resulting from excessive heat accumulation during/after laser irradiation), and even more serious thermal damage was found with increases in incident radiant exposure. As shown in Fig. 4(b), some ablation debris accumulated on the bottom of the incision can be clearly seen. By applying additional water layer to the
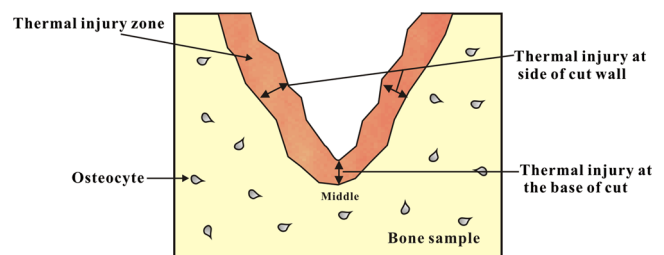

Fig. 3 Schematic of measurements of the zone of thermal injury at the base of the cut and the midpoint of each side of the ablated cut wall.

top surface of the tissue sample [Figs. 4(C), 4(c), 4(D), and 4(d)], the shape of the incision became more regular, smooth, and clean compared to the dry condition, and the zone of char formation and tissue denaturalization decreased significantly with a water layer of 0.8-mm thickness as shown in Fig. 4.

3.2 Geometry Measurement

The geometry measurements of cuts created on the bone sample as a function of water layer thickness at various incident radiant exposures are shown in Fig. 5. The error bars are the standard deviation of the data. In Fig. 5(a), the width of the osteotomy cut decreased monotonically with increasing water layer thickness when the fluence was below 32 J/cm^2, while with increasing radiant exposure (above 50 J/cm^2), the incision width curve presented a flat zone at water layer thickness less than 0.6 mm; that is, under these conditions, the additional water applied to the tissue surface had almost no influence on incision width. With additional water layer thickness (above 0.6 mm), the cut width decreased monotonically.

In Fig. 5(b), the cut depth (the distance from the top tissue surface to the cut bottom) decreased monotonically with increases in additional water layer thickness when the radiant exposure was less than 32 J/cm^2, and the deepest cut was obtained in the dry condition. When the radiant exposure was above 50 J/cm^2, with increasing water layer thickness, the cut depth showed a trend of first increasing and then decreasing, with the deepest cut at 0.4 mm for 50 and 70 J/cm^2, and 0.6 mm for 84 J/cm^2. Statistical analysis showed that the difference in cut depth was significant only when the thickness of additional water layer on the tissue surface was larger than 1.0 mm ($p < 0.05$).

3.3 Thermal Injury

The values of thermal injury thickness at both sides and the base of the osteotomy cut at various radiant exposures for dry and wet
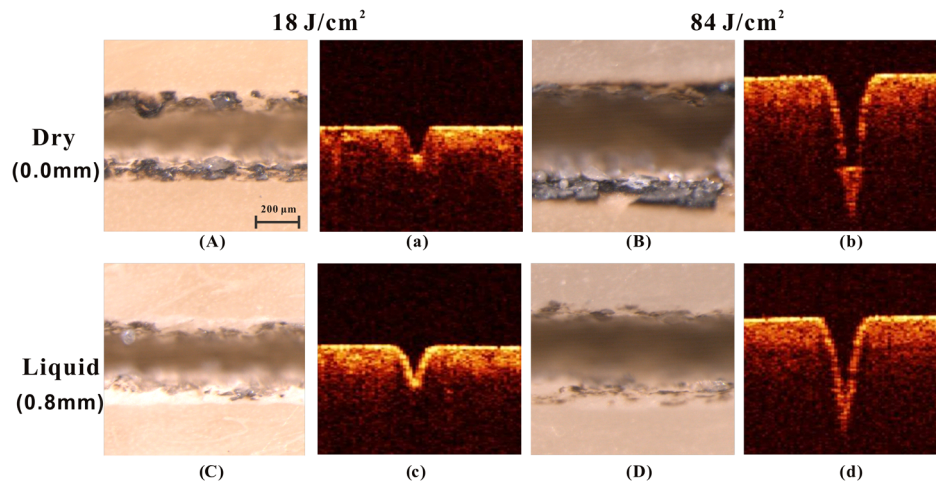

Fig. 4 Top stereomicroscope [(A) to (D)] and cross-sectional OCT [(a) to (d)] images of bone tissues ablated with pulse CO_2 laser at 18 [(A, a) and (C, c)] and 84 J/cm^2 [(B, b) and (D, d)] without [(A, a) and (B, b)] and with a water layer thickness of 0.8 mm [(C, c) and (D, d)], respectively.
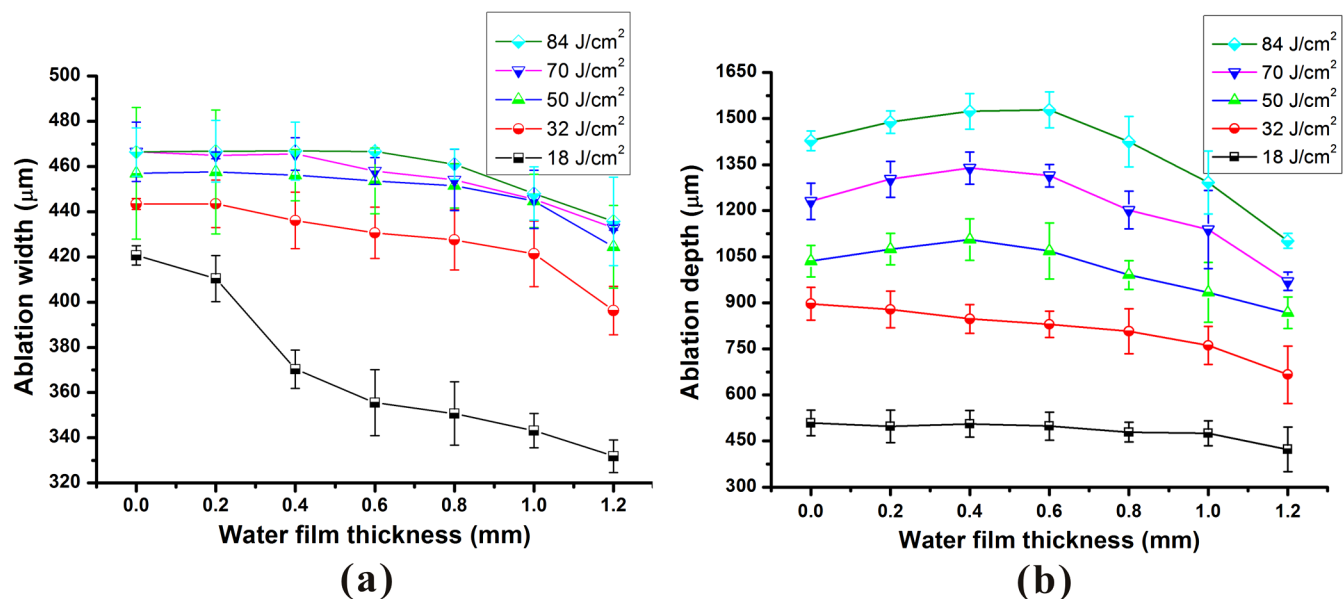

Fig. 5 Geometry measurements of osteotomy cut created on bovine shank bone with pulse CO_2 laser as a function of water layer thickness at various incident radiant exposures. (a) Cut width at the surface of bone sample, and (b) cut depth. The error bars are standard deviation of the data ($n = 8$).

ablation conditions are shown in Fig. 6. For the dry irradiation condition, the thickness of the thermal injury zone at both sides and the base of the osteotomy cut increased in severity with increasing incident radiant exposure because excessive heat accumulated during and after laser irradiation. The same feature can be observed for all wet irradiation conditions. The most thermal injury for both sides and the base of the osteotomy cut was produced in the dry ablation condition for all radiant exposures. By applying an additional water layer to the target tissue surface, the zone of thermal injury decreased significantly compared to the dry condition ($p < 0.05$) and reduced monotonically with increasing water layer thickness for all radiant exposures.

3.4 Microstructure Changes

Microstructure changes to the bone sample after irradiation by pulsed CO_2 laser at 50 J/cm^2 for dry and wet ablation conditions were evaluated with SEM and are presented in Fig. 7. Images A through C show the cut created on the bone tissue at a magnification of 200×; images a through c are 1000× magnifications of the corresponding white boxes outlined in A through C. For the dry ablation condition [Figs. 7(A) and 7(a)], the cut presented a corrugated or volcano-like profile with an irregular edge and rough surface. A loose smear layer covered the entire inner wall surface with bone debris attached on it, and large bone fragments accumulated randomly on the bottom of cut (indicated by the white arrow in Fig. 7(A). There was a transition layer of thermal injury between the irradiated site and untreated tissue. With increasing radiant exposure, the edge and inner wall surface of the cut became more irregular and rough, the altered layer enlarged, and char formation and cracks were found randomly along the cut. In contrast, the cut appearance after laser irradiation with a water layer of 0.4 mm showed a more regular profile with a sharp-cut edge and smooth inner wall surface [Figs. 7(B) and 7(b)], the altered layer significantly decreased, and no char formation or crack was found for all samples. However, upon further increasing the water layer up to 1.0 mm [Figs. 7(C) and 7(c)], the cut appearance became irregular and rough

with blocks of altered tissue [indicated by the red arrow in Fig. 7(c)] and melting matter [black arrow in Fig. 7(c)] attached on the inner wall, and a volume of bone debris accumulated on the base of the cut. Other radiant exposures tested in the study presented the same feature as mentioned above. The cut microstructure presents a trend of first becoming more and more regular and smooth with increasing water layer to a certain thickness, and then the regulation and smoothness of the ablation cut worsen more and more with further increases in water layer thickness. The finest cut appeared at different thicknesses of water layer for different radiant exposures. In the study, the finest cut, and also the deepest cut, appeared at 0.4 mm water thickness for 50 and 70 J/cm^2, and at 0.6 mm water thickness for 84 J/cm^2.

4 Discussion

The CO_2 laser has proved to be one of the most suitable candidates for bone surgery because of its strong absorption by the minerals of hard tissues, owing to the phosphate group of hydroxyapatite. Previous studies demonstrated a broad (up to several millimeters) zone of thermal injury around the laser cut with continuous (CW) and long-pulsed (pulse duration within the millisecond range) CO_2 laser ($\lambda = 10.6$ and 9.6 μm). Smaller thermal damage in bone and tooth tissue has been reported after application of short pulses (0.1 to 1 μs) of a transversely excited atmospheric pressure (TEA) or Q-switched CO_2 laser system. Ivanenko[26,27] observed an extremely narrow, 2- to 6-μm-thick thermally altered layer at the cut border in compacta and cartilage with pulse duration of about 0.3 μs. However, very high peak irradiances of several hundred megawatts per square centimeter are easily reached by focusing submicrosecond laser pulses from these laser systems. This leads to intense heating of the ablation debris, which continues to absorb the laser light after leaving the tissue, and finally to the formation of a plasma above the ablation site. The dense plasma can completely shield the tissue and so stop the tissue ablation, resulting in a low tissue ablation rate (5 to 10 μm/pulse). In combination with the limited pulse repetition rate for TEA lasers, this leads to a very low cutting speed, which of course is not suitable for
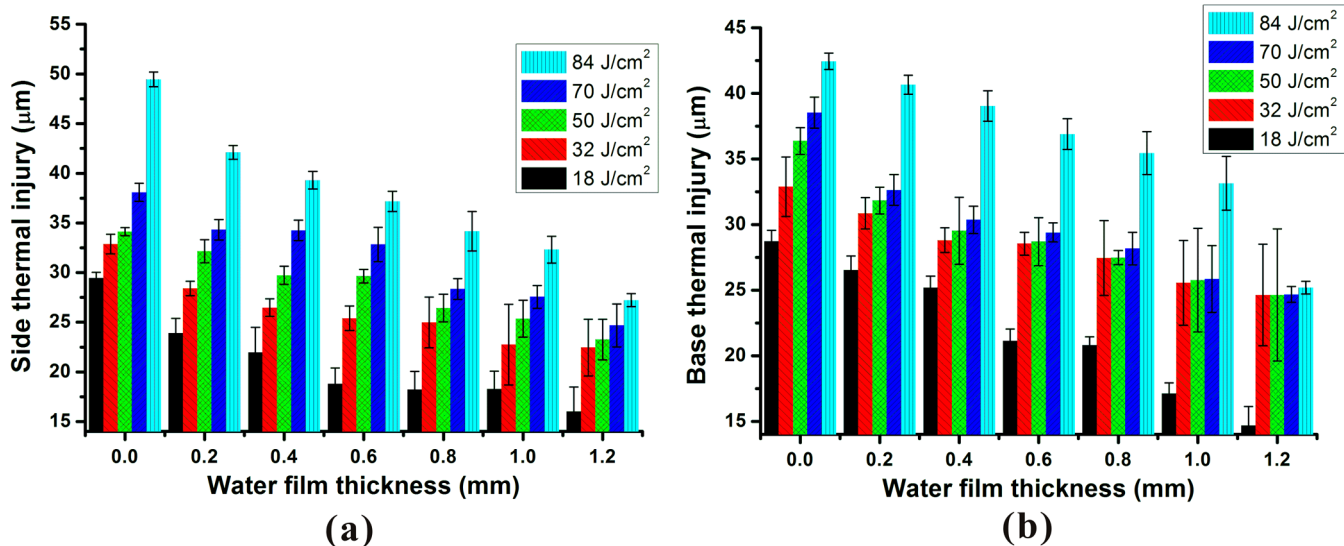

(a)

(b)

Fig. 6 The mean value of thermal injury thickness at both sides and the base of incision created on bovine shank bone after irradiation with pulse CO_2 laser at various incident radiant exposures versus water film thickness. (a) Thermal injury thickness at both sides, and (b) thermal injury on the base. The error bars are standard deviation of the data ($n = 6$).
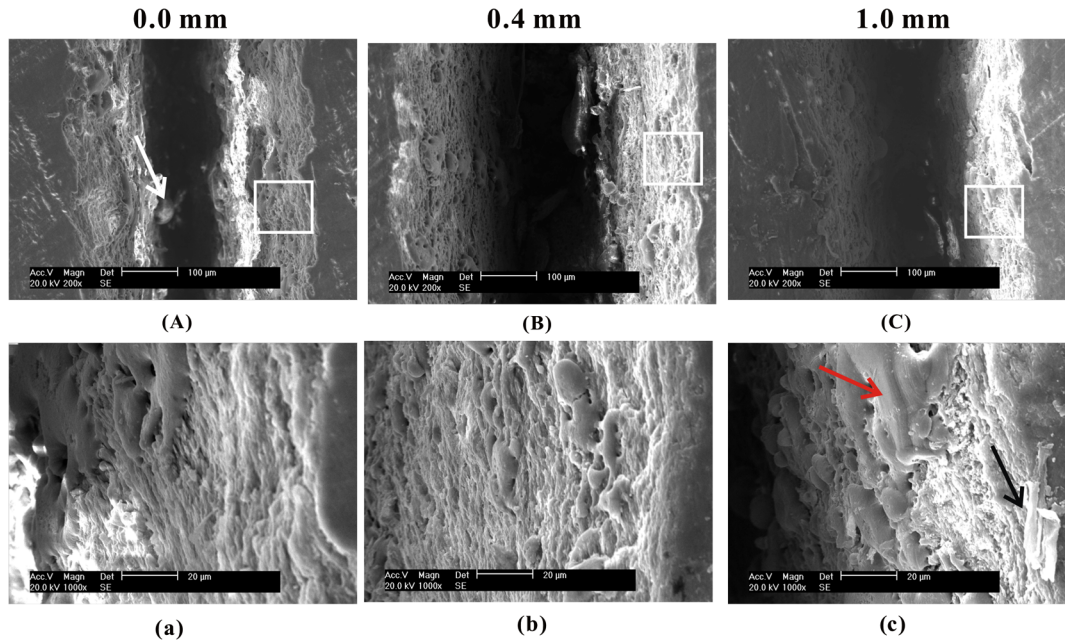
Fig. 7 Microstructural changes of osteotomy cut created on bovine shank bone by pulse CO_2 laser at 50 J/cm^2 for dry ablation condition (A) and wet ablation conditions with a water layer thickness of 0.4 mm (B) and 1.0 mm (C), respectively. Images (A) through (C) show the cut at a magnification of 200×; images (a) through (c) are 1000× magnifications of the corresponding white boxes outlined in (A) through (C).

bone surgery in clinical practice. In contrast, the relatively "long" CO_2 laser pulses with 100 μs are not only weaker plasma builders, which make it possible to focus the light beam in a much smaller spot, but may also provide high pulse energy at repetition rates of 1 to 10,000 Hz below the plasma-formation threshold and with very good and stable beam quality as compared to other laser systems. Therefore, by combining fast multi-pass beam scanning and the use of sprayed water, the relatively long ($\sim$100 μs) CO_2 laser pulses are able to produce very "clean" incisions in bone tissue with a much higher ablation rate (100 μm/pulse), more than an order of magnitude as compared to a TEA or Q-switched system.[3,28]

The data in available literature demonstrate strong variation in hard tissue absorption at CO_2 laser wavelengths of 9.2 to 11 μm. The absorption depth of 9.3 or 9.6 μm photons in dentin is 1 to 2 μm (bone should be similar), while at 10.6 μm, the absorption depth is 12 μm.[29] Therefore, more strongly absorbed wavelengths of 9.3 or 9.6 μm are suggested as being better suited for hard tissue ablation than 10.6 μm. For the short pulses (submicrosecond), the ablation rate and efficiency are much higher for 9.3 or 9.6 μm than for 10.6 μm.[29–31] However, when it is necessary to increase the ablation rate by using a pulse duration greater than 50 to 100 μs to avoid plasma shielding effects and excessive acoustic effects, the influence of wavelength tuning on the ablation of hard tissue would be less evident as the thermal diffusion length approaches 10 μm or greater for longer pulses. Scholz[32] reported for the laser pulse duration of 130 μs about a 70% higher ablation rate of compacta at the wavelength of 10.6 μm as compared to 9.6 mm. Ivanenko et al.[3] demonstrated that no significant difference was observed between 9.6 and 10.6 μm laser wavelengths by a pulse duration of 225 μs. In studies by the same group, a high-repetition-rate, 40 W, RF-excited CO_2 laser operating at 10.6 μm was used with pulse duration of 80 μs at repetition rates of 200 and 400 Hz to cut bone *in vivo* in an animal study to produce incisions without carbonization.[33]

The results of the present study showed that the high ablation rate needed for high speed bone cutting or osteotomy in bone surgery, greater than 100 μm/pulse, can be obtained easily by using a pulsed CO_2 laser operating at 10.6 μm with pulse duration of about 100 μs. Combined with multipass beam scanning and the use of additional water layer, thermal injury around the cut wall can be reduced to a tolerable level, comparable to that achieved by a diamond saw. Figure 4 shows that irregular surface modification and severe thermal damage (carbonization, charring, and cracking) were associated with dry ablation as a result of excessive heat accumulation. According to Rosa,[34] the "brown layer" indicates the loss of water and amide bands, while the carbonate and phosphate mineral bands remain unchanged. These types of thermal changes are expected for temperature excursions not exceeding 200 to 300°C. In the "black char layer," however, all the protein and water are removed, and there is significant modification of the mineral phase with loss of carbonate and disproportionation of hydroxyapatite to form other calcium phosphate phases. By applying an additional water layer to the tissue surface, the shape of the incision becomes more regular, smooth, and clean as compared to the dry condition because of the cooling effect of the water. Histological examination showed that the additional water layer significantly reduced the thickness of the thermal injury zone at both sides and the base of the ablation cut (as shown in Fig. 6). Since the thermal conductivity of water (0.611 W/m · K) is approximately 30 times greater than that of air (0.0267 W/m · K),[35] more thermal energy is possibly transferred to the water layer, cooling the target tissue surface via vaporization and convection processes. Moreover, the bubble motion in the liquid during laser irradiation may also contribute to the removal of ablated particles redeposited in the cut and reduces the oxidation of debris, which leads to clean and precise laser machining.

Since the room temperature absorption coefficient of water for erbium lasers ($\mu_a = 12480$ cm^{-1} at 2.94 μm)[21] is an order of

magnitude larger than that for CO_2 laser ($\mu_a = 817$ cm^{-1} at 10.6 μm),[14] we do not expect the additional water layer to have the same profound impacts on ablation rate and efficiency with CO_2 lasers as with erbium lasers. Under the dry ablation condition, cut volume is determined for a Gaussian laser beam by the focus spot diameter and by the ratio of the pulse energy density to the tissue ablation threshold. Under the wet ablation condition, the strong absorption of CO_2 laser radiation by water reduces the energy actually impacted on target tissue, which may reduce the ablation volume. Perhaps this is the explanation for the cut width and depth of ablation cut decreasing monotonically with increasing water layer thickness at radiant exposures below 32 J/cm^2 in the present study (as shown in Fig. 5). However, it is interesting to note that with increasing radiant exposure, the cut depth showed a trend of first increasing and then decreasing with the deepest cut at 0.4 mm for 50 and 70 J/cm^2, and 0.6 mm for 84 J/cm^2. These features, presented in Fig. 5(b), indicated that the interdependence of the water layer thickness and the incident radiant exposure actually contributed to enhancing ablation rate and efficiency, or at least to maintaining the same ablation rate and efficiency as dry conditions. There is a critical thickness of water layer for a given radiant exposure at which the ablation rate and efficiency can be maximized. The strong absorption of CO_2 laser radiation might initiate a vaporization process, creating a water vapor channel in the water layer that adversely contributed to the successive light energy of pulses passing through the water layer and impacting on target tissue, since the steam, in contrast to liquid water, has 100 to 1000 times lower density as well as a low absorption coefficient.[36–38] That is, only the leading part of the light energy was strongly absorbed by water to form a water vapor channel. Most of the successive light energy transmitted though the water vapor channel with a low absorption coefficient and interacted with target tissue. Moreover, the forces associated with vapor channel formation and subsequent collapse of the vapor channel might remove any poorly attached nonapatite phases of modified bone that may adversely absorb incident light energy, resulting in a shielding effect and reducing the rate and efficiency of ablation significantly. In this case, the effects of the water vapor channel may complement the decrease in ablation rate resulting from energy loss absorbed by the water layer to maintain the same, or even enhance, the ablation rate compared to the dry ablation condition, depending on the optimal selection of both water layer thickness and radiant exposure. This mechanism of laser-water interaction can also be used to explain the microstructure changes of the cut surface shown in Fig. 7, where the finest cut appeared at a certain thickness of water layer for a given radiant exposure. It can also be extended to explain water-mediated ablation with erbium lasers.

Based on the phenomenological observations of the present study, we can also speculate about the mechanism of water interaction with hard tissue. In previous studies investigating the water effects on this procedure, different hypotheses, including cavitation bubbles, hydrokinetic effect, and apatite crystalline fragments, have been presented.[24,39,40] Although these hypotheses explain the smoother crater and higher ablation rate with erbium laser pulses, they cannot explain the influence of the interdependence of water layer thickness and incident radiant exposure on ablation rate, thermal injury, and microstructure of the cut walls. As reported by Kang et al.,[1] the hydrokinetic effect proposed by Riziou et al.,[40] in which water droplets in the water spray are accelerated by laser photons, can be easily ruled out, since there was no water spray, only a static water layer applied to a target surface in the present study. The maximum cavitation bubble radius in water induced by laser irradiation has been evaluated by Isselin et al.[41] and reported to be approximately 620 μm for Er,Cr:YSGG (2.79 μm) by Kang et al.[1] Perhaps the maximum cavitation bubble radius can be used as a condition for water vapor channel formation. Only when the water layer thickness is thinner than the maximum radius of the cavitation bubble can the water vapor channel be formed and the rest of the laser energy be delivered through the vapor channel. The results also indicated there is a minimum thickness of water layer below which the vapor channel cannot be formed. In the present study, the optimal thickness of the water layer ranged from 0.4 to 0.8 mm, depending on the incident radiant exposure selected, in which the desired ablation results can be obtained.

5 Conclusions

This study demonstrates the influence of the interdependence of water layer thickness and incident radiant exposure on ablation performance by using a relatively long pulsed CO_2 laser. The results showed that by applying an additional water layer on tissue surface, the geometry of the cut presented a more regular and clean shape and thermal injury was reduced. There is an optimal thickness of the water layer for a given radiant exposure at which maximum ablation rate can be obtained. The desired ablation result depends on the optimal selection of both water layer thickness and incident radiant exposure.

References

1. H. W. Kang, J. Oh, and A. J. Welch, "Investigations on laser hard tissue ablation under various environments," *Phys. Med. Biol.* **53**(12), 3381–3390 (2008).
2. J. J. Kuttenberger et al., "Computer-guided CO_2-laser osteotomy of the sheep tibia: technical prerequisites and first results," *Photomed. Laser Surg.* **26**(2), 129–136 (2008).
3. M. Ivanenko et al., "Ablation of hard bone tissue with pulsed CO_2 lasers," *Med. Laser Appl.* **20**(1), 13–23 (2005).
4. M. Frentzen et al., "Osteotomy with 80-μs CO_2 laser pulses—histological results," *Laser Med. Sci.* **18**(2), 119–124 (2003).
5. S. H. Chung and E. Mazur, "Surgical applications of femtosecond lasers," *J. Biophotonics* **2**(10), 557–572 (2009).
6. J. I. Youn, P. Sweet, and G. M. Peavy, "A comparison of mass removal, thermal injury, and crater morphology of cortical bone ablation using wavelengths 2.79, 2.9, 6.1, and 6.45 microm," *Lasers Surg. Med.* **39**(4), 332–340 (2007).
7. J. I. Youn et al., "Mid-IR laser ablation of articular and fibro-cartilage: a wavelength dependence study of thermal injury and crater morphology," *Lasers Surg. Med.* **38**(3), 218–228 (2006).
8. B. Ivanov et al., "Mid-infrared laser ablation of a hard biocomposite material: mechanistic studies of pulse duration and interface effects," *Appl. Surf. Sci.* **208**(3), 77–84 (2003).
9. N. M. Fried and D. Fried, "Comparison of Er:YAG and 9.6-microm TE CO(2) lasers for ablation of skull tissue," *Lasers Surg. Med.* **28**(4), 335–343 (2001).

10. M. Stanislawki et al., "Hard tissue ablation with a free running Er:YAG and a Q-switched CO_2 laser: a comparative study," *Appl. Phys. B: Lasers Opt.* **72**(1), 115–120 (2001).
11. P. Spencer et al., "Effective laser ablation of bone based on the absorption characteristics of water and proteins," *J. Periodontol.* **70**(1), 68–74 (1999).
12. M. Buchelt et al., "Erb:YAG and Hol:YAG laser osteotomy: the effect of laser ablation on bone healing," *Laser Surg. Med.* **15**(4), 373–381 (1994).
13. J. A. Izatt et al., "Wavelength dependence of pulsed laser ablation of calcified tissue," *Laser Surg. Med.* **11**(3), 238–249 (1991).
14. M. Forrer et al., "Bone-ablation mechanism using CO_2 lasers of different pulse duration and wavelength," *Appl. Phys. B: Lasers Opt.* **56**(2), 104–112 (1993).
15. G. K. H. Eyrich, "Laser-osteotomy induced changes in bone," *Med. Laser Appl.* **20**(1), 25–36 (2005).
16. R. Hibst and U. Keller, "Effects of water spray and repetition rate on the temperature elevation during Er:YAG laser ablation of dentine," in *Medical Applications of Lasers III*, S. G. Bown et al., eds., pp. 139–144, SPIE, Barcelona, Spain (1996).
17. S. R. Visuri, J. T. Walsh, Jr., and H. A. Wigdor, "Erbium laser ablation of dental hard tissue: effect of water cooling," *Laser Surg. Med.* **18**(3), 294–300 (1996).
18. J. Meister et al., "Influence of the water content in dental enamel and dentin on ablation with erbium YAG and erbium YSGG lasers," *J. Biomed Opt.* **11**(3), 34030 (2006).
19. H. W. Kang, "Enhancement of high power pulsed laser ablation and biological hard tissue applications," The University of Texas at Austin (2006).
20. M. Staninec et al., "Influence of an optically thick water layer on the bond-strength of composite resin to dental enamel after IR laser ablation," *Lasers Surg. Med.* **33**(4), 264–269 (2003).
21. G. M. Hale and M. R. Querry, "Optical constants of water in the 200-nm to 200-μm wavelength region," *Appl. Optics* **12**(3), 555–563 (1973).
22. J. D. Featherstone and D. Fried, "Fundamental interactions of lasers with dental hard tissues," *Med. Laser Appl.* **16**(3), 181–194 (2001).
23. M. M. Ivanenko and P. Hering, "Wet bone ablation with mechanically Q-switched high-repetition-rate CO_2 laser," *Appl. Phys. B: Lasers Opt.* **67**(3), 395–397 (1998).
24. D. Fried et al., "Mechanism of water augmentation during IR laser ablation of dental enamel," *Lasers Surg. Med.* **31**(3), 186–193 (2002).
25. V. Colucci et al., "Water flow on erbium:yttrium-aluminum-garnet laser irradiation: effects on dental tissues," *Laser Med. Sci.* **24**(5), 811–818 (2009).
26. M. M. Ivanenko et al., "Bone tissue ablation with sub-μs pulses of a Q-switch CO_2 laser: histological examination of thermal side effects," *Laser Med. Sci.* **17**(4), 258–264 (2002).
27. M. M. Ivanenko et al., "In vitro incision of bone tissue with a Q-Switch CO_2 laser: histological examination," *Lasers Life Sci.* **9**, 171–179 (2000).
28. M. Staninec et al., "Pulpal effects of enamel ablation with a microsecond pulsed $\lambda = 9.3\ \mu$m CO_2 laser," *Lasers Surg. Med.* **41**(4), 256–263 (2009).
29. K. Fan, P. Bell, and D. Fried, "Rapid and conservative ablation and modification of enamel, dentin, and alveolar bone using a high repetition rate transverse excited atmospheric pressure CO_2 laser operating at lambda = 9.3 μm," *J. Biomed. Opt.* **11**(6), 64008–64011 (2006).
30. D. Fried et al., "Permanent and transient changes in the reflectance of CO_2 laser-irradiated dental hard tissues at l = 9.3, 9.6, 10.3, 10.6 mm and at fluences of 1–20 J/cm^2," *Lasers Surg. Med.* **20**(1), 22–31 (1997).
31. K. K. Sheth et al., "Selective targeting of protein, water, and mineral in dentin using UV and IR pulse lasers: the effect on the bond strength to composite restorative materials," *Lasers Surg. Med.* **35**(4), 245–253 (2004).
32. C. Scholz and Laser-Medizin-Zentrum, *Neue Verfahren der Bearbeitung von Hartgewebe in der Medizin mit dem Laser*, Ecomed (1992).
33. M. Ivanenko et al., "In vivo animal trials with a scanning CO_2 laser osteotome," *Lasers Surg. Med.* **37**(2), 144–148 (2005).
34. R. A. Dela et al., "Peripheral thermal and mechanical damage to dentin with microsecond and sub-microsecond 9.6 μm, 2.79 μm, and 0.355 μm laser pulses," *Lasers Surg. Med.* **35**(3), 214–228 (2004).
35. H. W. Kang et al., "Enhancement of bovine bone ablation assisted by a transparent liquid layer on a target surface," *IEEE J. Quant. Electron.* **42**(7), 633–642 (2006).
36. M. Mir et al., "Visualising the procedures in the influence of water on the ablation of dental hard tissue with erbium: yttrium—aluminium—garnet and erbium, chromium: yttrium—scandium—gallium-garnet laser pulses," *Laser Med. Sci.* **24**(3), 365–374 (2009).
37. R. J. Scammon et al., "Simulations of shock waves and cavitation bubbles produced in water by picosecond and nanosecond laser pulses," *Proc. SPIE* **3254**, 264 (1998).
38. E. D. Jansen et al., "Laser—tissue interaction during transmyocardial laser revascularization," *Ann. Thorac. Surg.* **63**(3), 640–647 (1997).
39. I. M. Rizoiu, A. I. Kimmel, and L. R. Eversole, "Effects of an Er, Cr: YSGG laser on canine oral hard tissues," *Proc. SPIE* **2922**, 74–83 (1996).
40. I. M. Rizoiu and L. G. DeShazer, "New laser-matter interaction concept to enhance hard tissue cutting efficiency," *Proc. SPIE*, **2134A**, 309–317 (1994).
41. J. C. Isselin, A. P. Alloncle, and M. Autric, "On laser induced single bubble near a solid boundary: contribution to the understanding of erosion phenomena," *J. Appl. Phys.* **84**(10), 5766–5771 (1998).